Available online at www.sciencedirect.com

SciVerse ScienceDirect

Procedia Environmental Sciences 10 (2011) 2042 – 2049

Procedia Environmental Sciences

2011 3rd International Conference on Environmental Science and Information Application Technology (ESIAT 2011)

Application of HJ-1B Data in Monitoring Water Surface Temperature

Ke Hu[1, 2], Feng Chen[3, 4, *], Shengwen Liang[2]

1, School of Resources and Environmental Science, Wuhan University, Wuhan 430079, China
2, Wuhan Environmental Monitoring Center, Wuhan 430015, China
3, Key Lab of Urban Environment and Health, Institute of Urban Environment, Chinese Academy of Sciences, Xiamen 361021, China
4. Xiamen Key Lab of Urban Metabolism, Xiamen 361021, China
my.li@sohu.com

Abstract

The water surface temperature (WST) regarded as an important indicator of water environment, have been obtained from remotely sensed thermal data widely. One thermal band of the new HJ-1B satellite, provided with relatively both high temporal and spatial resolution may provide us a good chance for water thermal dynamic study. The suitability of HJ-1B data was evaluated, in simultaneously obtaining WST for large area, through a case study in Wuhan city. WSTs retrieved by different methods were compared with the MOD 11 product and the in situ measurements. Validation results show that more accurate result was obtained by using the revised single channel (Re_SC) algorithm, with the root mean square error (RMSE) and systematic error (SE) were 0.73K and -0.17K compared with the MOD 11. Its' advantages in spatial and temporal resolution make the HJ-1B imageries to be an useful data source for monitoring water environment, as far as some related issues are resolved properly.

Keywords: thermal remote sensing, HJ-1B satellite, water surface temperature, Wuhan city

1.Introduction

It is well recognized that water is the source of life, and the terrestrial surface water is an important part of the water cycle. As stated in the document organized by the National Research Council (NRC, USA), water is essential to life for humans and their food crops, and for ecosystems [1], furthermore ,water temperature is important to many resource management and environmental fields [2]. Conventionally, monitoring the water temperature of lakes and rivers are based on the *in situ* measurement, but with a small number of samples or locations. This traditional way can only report the localized thermal conditions although the measurements are accurate. Nevertheless, remotely sensed imagery has

doi:10.1016/j.proenv.2011.09.320

advantages of the macroscopic and real-time access to water system dynamics, providing a suitable chance for monitoring tempo-spatial changes of water surface temperature [2]. Currently, in China, two new satellites named HJ-1A and HJ-1B were launched on September 6th, 2008, being intended for environment and disaster monitoring and forecasting. The infrared scanner (IRS) on board HJ-1B satellite has one thermal band (10.5~12.5 μm), of which the radiometric resolution is better than 1.0 K. The nadir spatial resolution of the thermal band is 300 m and the swath width is 720 km，thus with a four days repeat cycle [3].

The purpose of this study is to evaluate the potential of HJ-1B data for monitoring water temperature through suitable methods, thus to demonstrate the advantage in high temporal and spatial resolution for water resources dynamic assessment. Wuhan city, with a large proportion of water, was selected for a case study.

Methods

The Radiative Transfer Equation (RTE) applied to a particular wavelength (λ) in the thermal infrared region can be expressed in a simplified form:

$$L_\lambda^{sensor} = \left\{ \varepsilon_\lambda B_\lambda(T_s) + (1-\varepsilon_\lambda) L_\lambda^{\downarrow} \right\} \tau_\lambda + L_\lambda^{\uparrow} \quad . \qquad (1)$$

Where, τ_λ is the atmospheric transmissivity, $L_\lambda^{\uparrow}$ is the up-welling atmospheric radiance, $L_\lambda^{\downarrow}$ is the downwelling atmospheric radiance, ε_λ is the land surface emissivity, λ is the wavelength, T_s is the land surface temperature (LST) and $B_\lambda(T_s)$ is the blackbody radiance given by the Planck's law.These parameters are spectrally related, when taking into account a certain sensor band, magnitudes are integrated according to the relative spectral response (RSR) function of the thermal band.

2.1The revised single-channel algorithm

A generalized single-channel algorithm was developed by Jimenez-Munoz and Sobrino (2003), to retrieve LST from only one thermal band [4]:

$$T_s = \gamma \left[\frac{1}{\varepsilon} (\psi_1 L^{sensor} + \psi_2) + \psi_3 \right] + \delta \quad . \qquad (2)$$

with $$\gamma = \left[\frac{c_2 L^{sensor}}{T_{sensor}^2} \left(\frac{\lambda_{eff}^{\ 4}}{c_1} L^{sensor} + \frac{1}{\lambda_{eff}} \right) \right]^{-1} ,$$

$$\delta = T_{sensor} - \gamma L^{sensor}$$

Where, T_{sensor} is the at-sensor brightness temperature, λ_{eff} is the effective wavelength (Section: *Brightness temperature*), ψ_1 , ψ_2 and ψ_3 referred to as atmospheric functions (AFs), while $c_1 = 1.19104 \times 10^8$ Wμm^{4}m^{-2}sr^{-1} and $c_2 = 14387.7$ μmK .

The AFs are mainly dependent on atmospheric water vapor content (w) with a polynominal fit [4]. Duan *et al*. (2008) modified the coefficients in the AFs to revise the generalized single-channel method for obtaining LST from the thermal band of HJ-1B data [5]:

$$\psi_1 = 0.0412w^2 + 0.0936w + 0.9856, \quad \psi_2 = -0.7174w^2 - 0.8812w - 0.3941$$
$$\psi_3 = 0.2639w^2 + 0.6499w + 0.4703 \quad . (3)$$

2.2The revised mono-window algorithm

Qin *et al*. (2001) proposed the mono-window algorithm, exclusively for obtaining LST from Landsat TM [6]:

$$T_s = \left[a(1-C-D)+(b(1-C-D)+C+D)T_{sensor} - DT_a\right] / C \quad . \quad (4)$$
$$\text{with } C = \varepsilon\tau \,, D = (1-\tau)[1+(1-\varepsilon)\tau]$$

Where, a and b are empirical constants, T_a represents the mean atmospheric temperature, which can be estimated from the near-surface air temperature (T_0).

Duan *et al*. (2008) made adjustments to these coefficients and constants. Specifically, for the range of 0-70℃, $a = -68.035$ and $b = 0.46372$, while the atmospheric transmittance and mean atmospheric temperature (for Mid-latitude area) can be calculated by using [5]:

$$\tau = 0.9821 - 0.1241w \,. \quad (5)$$
$$T_a = 20.43072 + 0.905071T_0 \text{ (Summer)} \,, \quad T_a = 24.70005 + 0.88894T_0 \text{ (Winter)} \,. \quad (6)$$

2.3 Accuracy assessment

In this research, we compared the retrieved water surface temperature (WST) with the near time *in situ* measurements and the MODIS surface temperature product (MOD 11). Two types of error measurement :root mean square error (RMSE), systematic error (SE) , were used:

$$\text{RMSE} = \sqrt{\frac{\sum_{J=1}^{NN}(\text{WST}_J - \text{WST}_J^{'})^2}{NN}} \quad \text{and} \quad \text{SE} = \frac{\sum_{J=1}^{NN}(\text{WST}_J - \text{WST}_J^{'})}{NN} \,. \quad (7)$$

Where, WST_J is the retrieved WST of sample J , while $\text{WST}_J^{'}$ is the 'truth' for sample J recorded through *in situ* measurement or MOD11; and *NN* is the total number of samples for validation.

For MOD 11 product, the MODIS pixels were selected, which were covering the HJ-1B pixels inside with small WST variations (Fig.1(a)). In this paper the variation threshold (Th) was set as 0.5 K. For each selected MODIS pixel, the corresponding HJ-1B pixels covering the same area were chosen, and the mean temperature of them was calculated as the retrieved value (served as WST_J in Eq. (7)). Meanwhile,

for *in situ* measurements, a sampling unit of 3×3 pixels (Fig.1(b)) was used to avoid the effects of geometric errors between HJ-1B and *in situ* measurements.

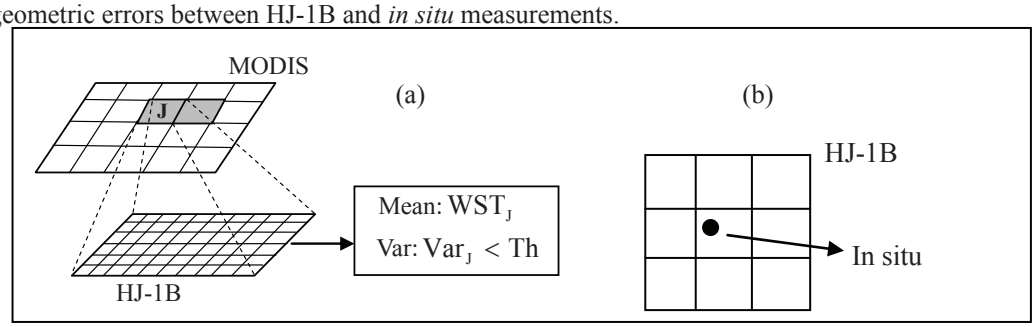

Figure1 Conceptual procedure of sampling pixels for validation

3. Study area and datasets

3.1 Study area and data sets

Wuhan located in central China, is the capital of Hubei Province. The Yangtze, World's third longest river and its largest tributary Hanshui meet in Wuhan and cut the city into three parts (Hankou, Hanyang and Wuchang). As a typical garden city featuring mountains and waters, Wuhan is home to hundreds of hills and nearly 200 lakes of various sizes. With a water area making up 25.8% of its entire territory, Wuhan is ranked the first among major Chinese cities in water resources. East Lake is China's biggest downtown lake covering an area of 33km^2 [7].

In this paper, data sets include one HJ-1B IRS image (path/row 455/77) and one CCD2 image (path/row 455/80), acquired on 31 November, 2010. Collection time was around 11:02 (Beijing Time), specifically 11: 01:44 ~11:02:36 and 11:00:44 ~11:02:23 for CCD2 and IRS respectively.

3.2 Atmospheric products

Our previous researches demonstrated the atmospheric heterogeneity at regional scale and advocated that it is vital to get atmospheric parameters properly to precisely retrieve LST, especially for sensors provided with only one thermal infrared band[8]. Because Terra MODIS passes over our study area more or less at the same time as HJ-1B does, the standard atmospheric products (MOD 07 and MOD 05[9]) were selected to extract the atmospheric variables. The effectiveness of the standard products in atmospheric correction for the infrared thermal bands has been demonstrated in previous researches [10-11]. A method for extracting the atmospheric variables (near surface air temperature and water vapor content) from the standard atmospheric products was discussed [11].

3.3 Data processing

3.3.1 Pre-processing

These HJ-1B images were co-registered by treating one near time SLC-off Landsat ETM+ image as the geometric reference. The error of rectification was within 0.5 pixels in this study. All data involved in this study were co-registered in the same coordinate system (UTM/WGS84, N50). According to the calibration procedure suggested by CRESDA [15], radiometric correction was conducted for band2 and

band4 of CCD2 . However, absolute radiometric correction for atmospheric influence was not conducted due to the non-availability to the real-time atmospheric profiles.

3.3.2 Brightness temperature

Generally, the procedure for obtaining brightness temperature (BT) from the thermal infrared band of HJ-1B IRS includes radiometric correction (Eq. (8)) and BT inversion. Radiances recorded by the satellite sensor are normalized values weighted by its channel's RSR function. A suitablely representative wavelength is necessary for the BT inversion process, when there are no referenced correction coefficients [12]. In this case, the BT results can be estimated by using Eq. (9):

$$L^{sensor} = (DN - bias) / gains . \tag{8}$$

$$T_{BT} = \frac{c_2}{\lambda_{eff} \ln(\frac{c_1}{L^{sensor} \lambda_{eff}^{5}} + 1)} . \tag{9}$$

Where, $gains$ and $bias$ can be obtained from the header file or provided by CRESDA periodically. In this paper, λ_{eff} (11.576 μm) was estimated through trapezoidal numerical integration [12].

3.3.3 Emissivity

As mentioned previously (in Section: *Methods*), for retrieving surface temperature from one thermal band, the emissivity is a required parameter no matter which retrieval method is used. In this study, classiffication approach is rational when water area is focused exclusively, due to its homogeneity compared with other land use/cover classes. Generally, the emissivity estimation procedure includes: identifying all water bodies and assigning an identically representative emissivity to them. The water body is identified by means of threshold segmentation of the normalized difference water index (NDWI [13]), and the threshold value was selected through interactive way. Water emissivity was estimated by means of using the mean value for several typical water sample types included in MODIS UCSB emissivity library [14] and filtered according to the RSR function.

4. Results and discussion

We compared the estimated WSTs (using Re_SC and Re_MW) and the BTs with the MOD11 product. Validation results (Table 1) show that WSTs were more accurately by means of these revised retrieval methods, compared with the BT obtained directly from the at-sensor radiance. The Re_SC algorithm performed better than the Re_MW algorithm, which might be associated with the uncertainties of variables extracted from MODIS atmospheric products.

Table 1 Accuracy assessment compared with MOD 11 [K]

	BT	Re_SC	Re_MW
RMSE	4.07	0.73	3.00
SE	-4.00	-0.17	-2.90

Compared with the *in situ* measurements (Fig.2(a)), overestimated WSTs were obtained by Re_SC, whereas the results obtained by Re_MW were more proximate to the *in situ* records with slight underestimated bias. BTs are significantly less than the *in situ* measurements. These findings may also be consistent with the previous validation results (Table 1). Usually, radiance recorded by the satellite sensor is mainly related to its surface thermal conditions, with the depth being less than 0.1mm [2], so the retrieved WST mainly indicates the characteristics of water surface. However, the *in situ* measurement reflects the thermal condition at depth of water. For autumn season, especially approximate to noon (around 11:00 am), water surface is always warmer than the part underneath. In this case, the remotely sensed WSTs are relatively higher than the nearly simultaneous *in situ* ones, without regard to the uncertainties caused by the sampling scale difference and the temporal intervals.

There is a good relationship between the estimated WST result and the MOD11 product(Fig.2(b)). Obviously, most samples with low or medium temperature (less than 293 K) are locating around the neighborhood of the 1:1 line, whereas for warmer regions the retrieved results from HJ-1B data were more likely underestimated. These obvious discrepancies may be associated with the mixed pixel issue [2]. Therefore, more details should be explored in depth.

Compared with the MOD 11 product, the spatial distribution of WST obtained by Re_SC method is showing with details (Fig.3). The Yangtze River (also called Changjiang) is exhibiting the warmest condition, as well as the Hanshui (also called Hangjiang). Taking the East Lake for example (the enlarged part in Fig.3), the limited *in situ* measurements are unable to completely indicate thermal conditions of the complex lake system. Therefore, it should be a profitable way for water monitoring, that is combing WST maps derived from remotely sensed thermal imagery with *in situ* temperature measurements. This integration provides a near-contiguous dataset of the water temperature at the surface and at depth through time [2].

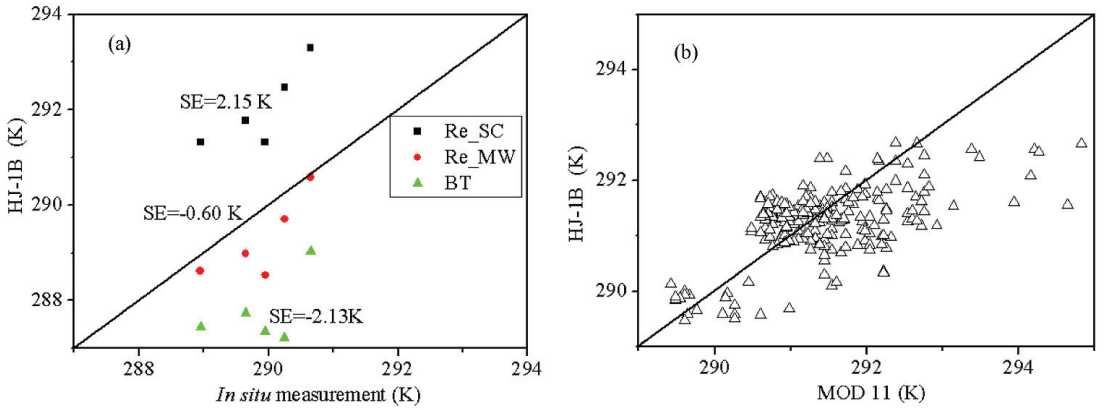

Figure 2 Comparison analysis: (a)between the retrieved WST and the *in situ* measurements for samples of East Lake; and (b) the retrieved WST (using the Re_SC method) vs the MOD11.

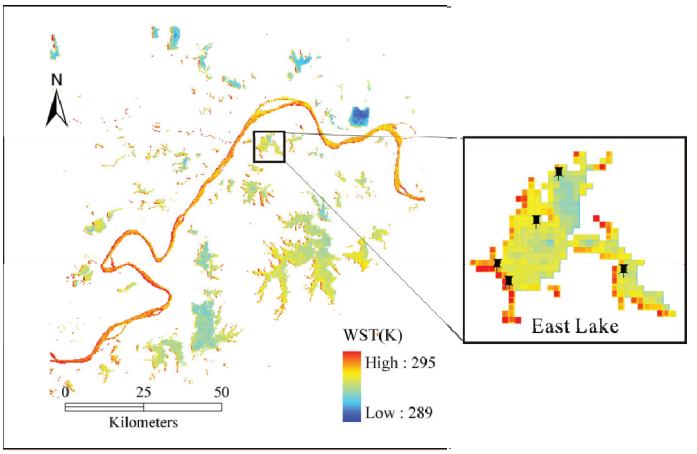

Figure 3 Spatial distribution of WST obtained from HJ-1B data by using Re_SC method

5. Conclusion

Taking Wuhan city as the interested area, we discussed the potential capacity of HJ-1B data for monitoring water temperature. Retrieval methodology is needed to be improved, although rational results were obtained. For example, an effective wavelength was used for estimating brightness temperature, which probably introduced errors into the final results. Retrieval errors caused by the uncertainty of atmospheric products should be discussed in depth. Problems associated with mixed pixels combing 'water' and 'no water' did significantly impact the retrieval procedure and results, and further researches should be conducted to resolve this issue. In addition, the map of water resources was identified according to NDWI with a suitable threshold; however, more effective methods will be developed. In conclusion, given the improvements mentioned above are made, the HJ-1B imageries should be one of data sources for water environment monitoring with high spatial and temporal resolution.

Acknowledgement

This study was supported partially by the Knowledge Innovation Program of Chinese Academy of Sciences, CAS (Grant No. 09L4401D10). Miss. Yuanyuan Zhang, Mr. Wei He and Mr. Aichun Wang of CRESDA gave useful advices on HJ-1B image processing. We thank CRESDA and USGS for providing freely HJ-1B and SLC-off Landsat ETM+ data respectively. Appreciations are given to the NASA for providing the MODIS land and atmospheric products.

References

[1] National Research Council: Integrating Multiscale Observations of U.S. Waters. National Academy of Sciences (2008), NW Washington.

[2] G. I. Sentlinger, S.J. Hook, and B. Laval: Sub-pixel water temperature estimation from thermal-infrared imagery using vectorized lake features. Remote Sensing of Environment, Vol.112(4)(2008), p.1678-1688.

[3] Information on http://www.cresda.com/n16/n1130/n1582/8384.html.

[4] J. C. Jimenez-Munoz and J. A. Sobrino: A generalized single-channel method for retrieving land surface temperature from remote sensing data. Journal of Geophysical Research, Vol.108(D22)(2003), p.4688.

[5] S.B. Duan, G. J. Yuan, Y. G. Qian, Z.L.Li, X.G. Jiang, and Xiao.W. Li: Two single-channel algorithms for retrieving land surface temperature from simulated HJ-1B data. Progress in Natural Science, Vol.18(9)(2008), p.1001-1008.

[6] Z. Qin, A. Karnieli and P. Berliner: A mono-window algorithm for retrieving land surface temperature from Landsat TM data and its application to the Israel-Egypt border region. International Journal of Remote Sensing, Vol.22(18)(2001), p.3719-3746.

[7] Information on http://www.wuhan.gov.cn.

[8] F. Chen, Y. Z. Xiong, S. P. Huang and H.Ye: Spatial Heterogeneity of Atmospheric Water Vapor and Its Influence on the Retrieval of Land Surface Temperature Based on Remote Sensing Data. Remote Sensing for Land & Resources, Vol.(2) (2010), p.35-40.

[9] Information on http://modis-atmos.gsfc.nasa.gov/products.html.

[10] J. C. Jimenez-Munoz, J. A. Sobrino, C. Mattar and B. Franch: Atmospheric correction of optical imagery from MODIS and Reanalysis atmospheric products. Remote Sensing of Environment, Vol.114(2010), p.2195-2210.

[11] F. Chen, X.F. Zhao, H. Ye and H.Y.Hu: Retrieving Land Surface Temperature from Landsat TM Using Different Atmospheric Products as Ancillary Data. ICSDM2011 & Bj-IWGIS, Fuzhou, China, 2011(Accepted).

[12] H.Y.Hu, F. Chen and Q. C. Wang: Estimating the Effective Wavelength of the Thermal Band for Accurate Brightness Temperature Retrieval：Methods and Comparison. ICSDM2011 & Bj-IWGIS, Fuzhou, China, 2011(Accepted).

[13] S. K. McFeeters: The Use of Normalized difference Water Index (NDWI) in the Delineation of Open Water Features. International Journal of Remote Sensing, Vol.17(7)(1996), p.1425-1432.

[14] Information on http://gicessucsbedu/modis/EMIS/html/emhtml.

[15] Information on http://www.cresda.com/n16/n1115/n1522/n2103/index.html.